

## Supplementary Information

### Copper and silver heterometallic iodoantimonates: structures, thermal stability and optical properties

Irina A. Shentseva<sup>a</sup>, Andrey N. Usoltsev<sup>a</sup>, Nikita A. Korobeynikov<sup>a</sup>, Maxim N. Sokolov<sup>a</sup> and Sergey A. Adonin\*<sup>a,b</sup>

<sup>a</sup> Nikolaev Institute of Inorganic Chemistry, Siberian Branch of Russian Academy of Sciences, Lavrentieva St. 3, 630090 Novosibirsk, Russian Federation

<sup>b</sup> Irkutsk Favorsky Institute of Chemistry Siberian Branch of Russian Academy of Sciences, 664033 Favorsky St. 1, Irkutsk, Russian Federation

FTIR spectra were measured on SCIMITAR FTS 2000 spectrometer with a resolution of 2 cm<sup>-1</sup> in the range of 400-4000 cm<sup>-1</sup>. Samples of **1-7** (around 1-2 mg) were mixed with dry KBr (around 100 mg), grounded in agate mortar, pressed under vacuum and placed into pellets for IR measurements.

#### NMR experiments

For <sup>1</sup>H-NMR spectra measurements samples of iodide salts were dissolved in approximately 800 μl of DMSO-D6 each and placed in NMR-tubes. All NMR experiments were performed on a Bruker Avance 500 (frequency 500.13 MHz) spectrometer at 25 °C.

All residual solvent and water signals (2.50 and 3.33 ppm respectively) were omitted.

**1,3-dimethylpyridinium iodide (1)**. 12 mg sample, (about 0.05 mmol). <sup>1</sup>H-NMR: δ = 8.93 (s, 1H), 8.84-8.82 (d, 1H), 8.44-8.43 (d, 1H), 8.05-8.03 (t, 1H), 4.32 (s, 3H), 2.09 (s, 3H) ppm.

**1,3,4-trimethylpyridinium iodide (2)** 12 mg sample (about 0.05 mmol). <sup>1</sup>H-NMR: δ = 8.80 (s, 1H), 8.72-8.70 (d, 1H) 7.93-7.92 (d, 1H), 4.25 (s, 3H), 2.39 (s, 3H), 2.10 (s, 3H) ppm.

**3-chloro-1-methylpyridinium iodide (3)** 13 mg sample, (about 0.05 mmol). <sup>1</sup>H-NMR: δ = 9.40 (s, 1H), 9.02-9.01 (d, 1H) 8.78-8.76 (d, 1H) 8.20-8.17(dd, 1H), 4.35 (s, 3H) ppm.

**3-bromo-1-methylpyridinium iodide (4)** 15 mg sample, (about 0.05 mmol). <sup>1</sup>H-NMR: δ = 9.43 (s, 1H), 9.04-9.03 (d, 1H), 8.87-8.85 (d, 1H), 8.11-8.08 (dd, 1H), 4.34 (s, 3H) ppm.

**(4-dimethylamino)-1-methylpyridinium iodide (5)** 13 mg sample, (about 0.05 mmol). <sup>1</sup>H-NMR 8.24-8.22 (d, 2H), 7.04-7.02 (d, 2H), 3.92 (s, 3H), 3.19 (s, 6H) ppm.

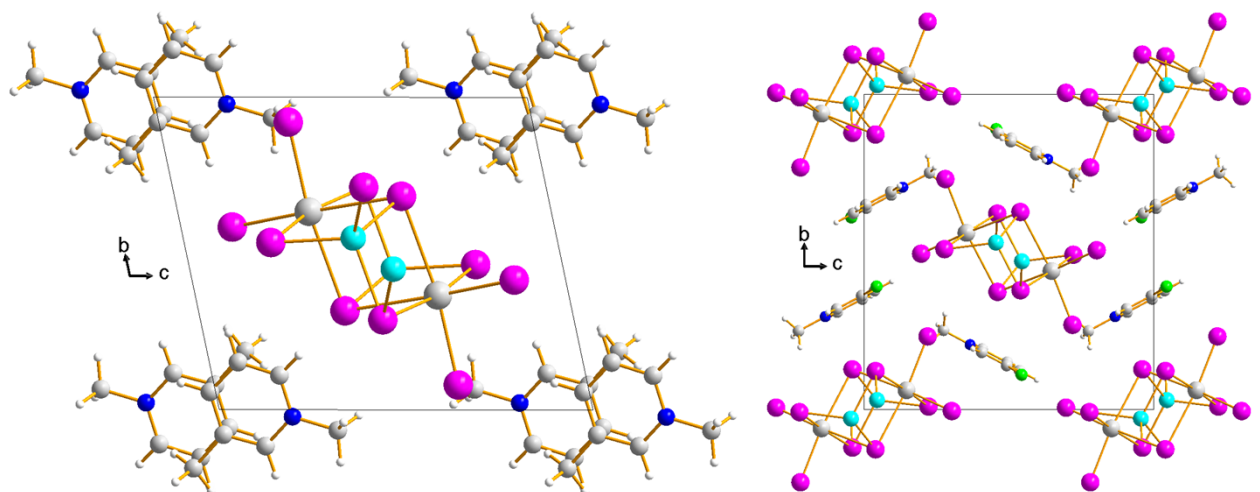


Figure S1. Crystal packing of **1** (left) and **3** (right) along  $\alpha$  axis. N blue, H white, C and Sb grey, Cu turquoise, I purple.

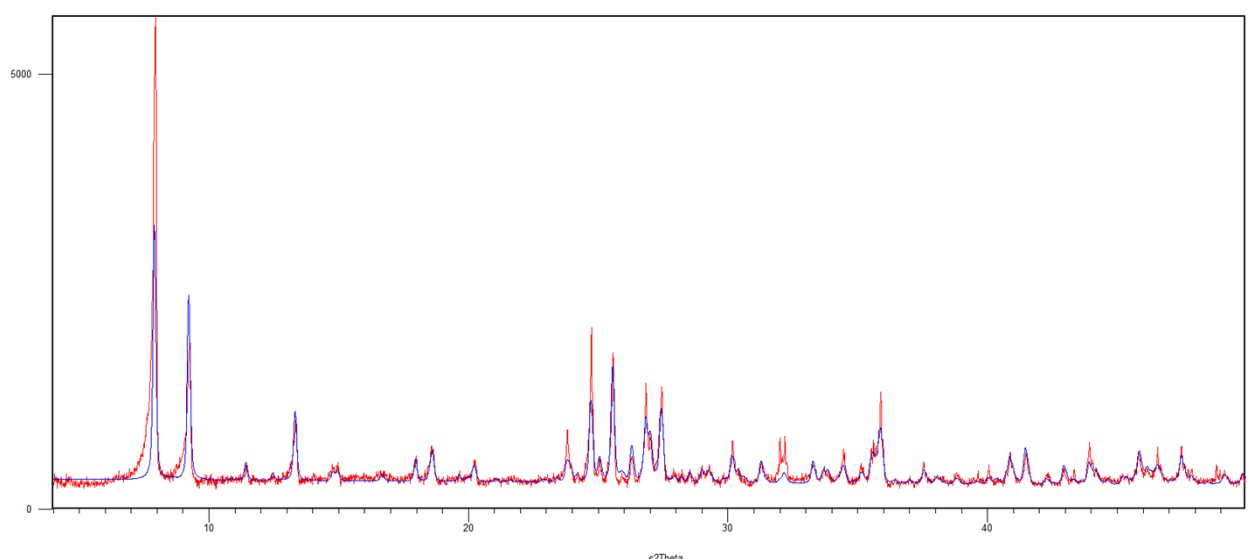


Figure S2. Experimental powder XRD of **1** (red) in comparison with the pattern simulated from single crystal X-ray data for **1** (black).

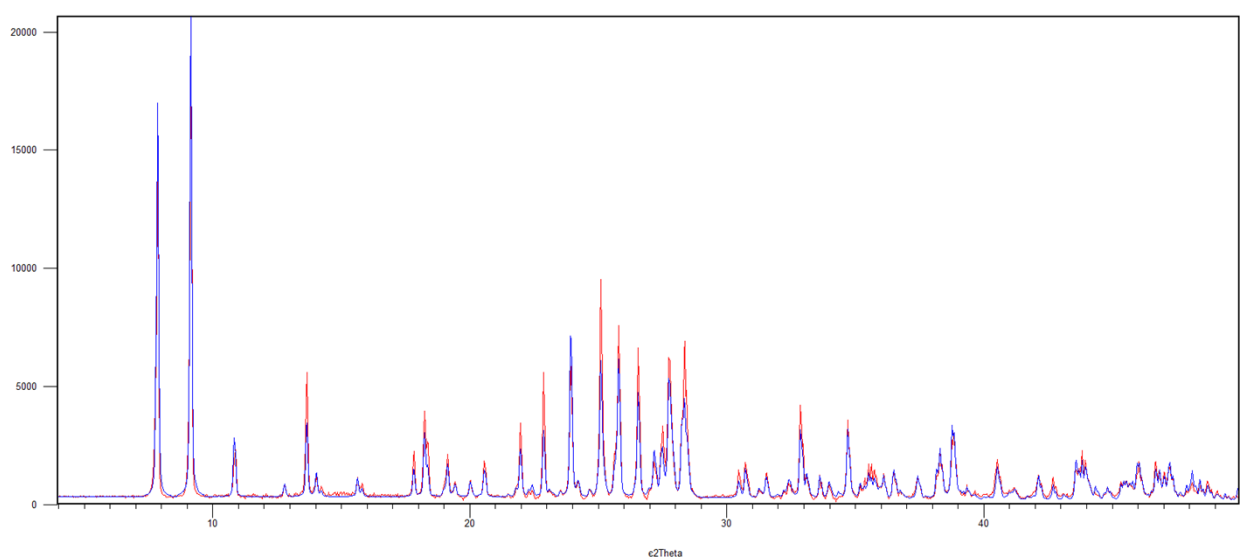


Figure S3. Experimental powder XRD of **2** (red) in comparison with the pattern simulated from single crystal X-ray data for **2** (black).

Table S1. Crystal data and structure refinement for compounds **1**-**7**.

Identification code	<b>1</b>	<b>2</b>	<b>3</b>	<b>4</b>	<b>5</b>	<b>6</b>	<b>7</b>
CCDC number							
Empirical formula	C <sub>7</sub> H <sub>10</sub> CuSbI <sub>5</sub> N	C <sub>8</sub> H <sub>12</sub> CuSbI <sub>5</sub> N	C <sub>6</sub> H <sub>7</sub> CuSbClI <sub>5</sub> N	C <sub>6</sub> H <sub>7</sub> CuSbBrI <sub>5</sub> N	C <sub>8</sub> H <sub>13</sub> CuSbI <sub>5</sub> N <sub>2</sub>	C <sub>8</sub> H <sub>20</sub> CuSbI <sub>5</sub> N	C <sub>8</sub> H <sub>20</sub> AgSbI <sub>5</sub> N
Formula weight	927.95	941.98	948.37	992.83	956.99	950.04	994.37
Temperature/K	150	150	150	150	150	296	150
Crystal system, space group	Triclinic, <i>P</i> - <i>I</i>	Triclinic, <i>P</i> - <i>I</i>	Monoclinic, <i>P</i> 2 <sub>1</sub> / <i>c</i>	Monoclinic, <i>P</i> 2 <sub>1</sub> / <i>c</i>	Triclinic, <i>P</i> - <i>I</i>	Triclinic, <i>P</i> - <i>I</i>	Triclinic, <i>P</i> - <i>I</i>
a/Å	8.0703(7)	8.2528(4)	8.1539(5)	8.1878(4)	8.0766(6)	8.5175(6)	8.8155(3)
b/Å	10.0900(8)	10.0963(4)	15.3736(9)	15.4248(7)	10.0734(8)	10.8315(9)	10.4685(4)
c/Å	11.4562(9)	11.6978(5)	14.6001(10)	14.6310(7)	13.1297(10)	11.3710(9)	11.2611(4)
$\alpha^{\circ}$	99.541(2)	105.739(2)	90	90	107.997(2)	93.316(3)	91.247(1)
$\beta^{\circ}$	96.768(3)	92.468(2)	103.809(2)	104.228(2)	97.929(2)	99.798(3)	100.681(1)
$\gamma^{\circ}$	105.795(2)	99.469(1)	90	90	104.914(2)	97.943(3)	96.806(1)
Volume/Å <sup>3</sup>	872.08(12)	921.41(7)	1777.29(19)	1791.14(15)	1371.3(3)	1020.27(14)	1013.01 (6)
Z	2	2	4	4	2	2	2
D <sub>calc</sub> g/cm <sup>3</sup>	3.534	3.395	3.544	3.682	3.332	3.092	3.260
$\mu/\text{mm}^{-1}$	11.594	10.976	11.53	13.52	10.61	9.91	9.90
F(000)	808	824	1648	1720	840	840	876
Crystal size/mm <sup>3</sup>	0.13 × 0.1 × 0.09	0.15 × 0.15 × 0.1	0.11 × 0.09 × 0.06	0.2 × 0.15 × 0.1	0.16 × 0.13 × 0.08	0.1 × 0.1 × 0.08	0.12 × 0.1 × 0.06
Tmin, Tmax	0.517, 0.746	0.461, 0.747	0.464, 0.746	0.567, 0.746	0.511, 0.746	0.608, 0.745	0.598, 0.747
2Θ range for data collection/°	5.028 to 61.096	4.758 to 66.300	5.144 to 63.074	5.132 to 54.238	4.534 to 59.252	3.810 to 52.930	3.684 to 66.452
Index ranges	-11 ≤ h ≤ 11, -14 ≤ k ≤ 14, -16 ≤ l ≤ 16	-12 ≤ h ≤ 12, -15 ≤ k ≤ 15, -17 ≤ l ≤ 17	-11 ≤ h ≤ 11, -22 ≤ k ≤ 22, -14 ≤ l ≤ 21	-10 ≤ h ≤ 10, -19 ≤ k ≤ 17, -18 ≤ l ≤ 18	-11 ≤ h ≤ 11, -14 ≤ k ≤ 13, -18 ≤ l ≤ 18	-7 ≤ h ≤ 10, -13 ≤ k ≤ 13, -14 ≤ l ≤ 14	-13 ≤ h ≤ 13, -16 ≤ k ≤ 16, -17 ≤ l ≤ 17
Diffractometer	Bruker D8 Venture	Bruker D8 Venture	Bruker D8 Venture	Bruker X8Apex	Bruker D8 Venture	Bruker Apex Duo	Bruker D8 Venture
R <sub>int</sub>	0.032	0.027	0.038	0.049	0.043	0.034	0.030
No. of measured, independent and observed [I > 2σ(I)] reflections	12992/5047/4810	19373/7012/6570	24400/5915/5447	17064/3954/3549	16437/5211/4988	9410/4119/3046	21976/7736/6363
Data/restraints/parameters	5047/0/139	7012/0/149	5915/0/137	3954/0/138	5211/0/158	4119/0/149	7736/0/150
Goodness-of-fit on F <sup>2</sup>	1.181	1.155	1.167	1.209	1.168	0.935	1.013
Final R indices [I>=2σ (I)]	R <sub>1</sub> = 0.0239, wR <sub>2</sub> = 0.0533	R <sub>1</sub> = 0.0192, wR <sub>2</sub> = 0.0417	R <sub>1</sub> = 0.0221, wR <sub>2</sub> = 0.0455	R <sub>1</sub> = 0.0411, wR <sub>2</sub> = 0.0588	R <sub>1</sub> = 0.0234, wR <sub>2</sub> = 0.0558	R <sub>1</sub> = 0.0312, wR <sub>2</sub> = 0.0517	R <sub>1</sub> = 0.0258, wR <sub>2</sub> = 0.0395
R indices [all data]	0.0255	0.0216	0.0257	0.0493	0.0249	0.0502	0.0381
(sin θ/λ) <sub>max</sub> (Å <sup>-1</sup> )	0.715	0.769	0.736	0.641	0.696	0.627	0.771
Largest diff. peak/hole/e/Å <sup>3</sup>	0.88/-0.73	0.90/-0.78	0.62/-1.13	0.94/-1.09	1.11/-0.65	0.86/-0.83	0.85/-0.80

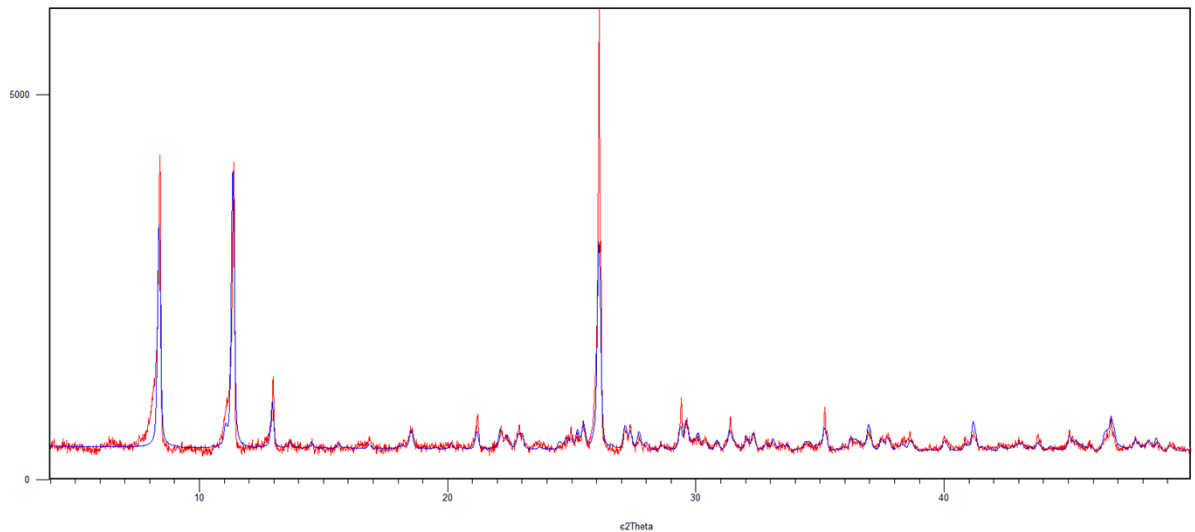


Figure S4. Experimental powder XRD of **3** (red) in comparison with the pattern simulated from single crystal X-ray data for **3** (black).

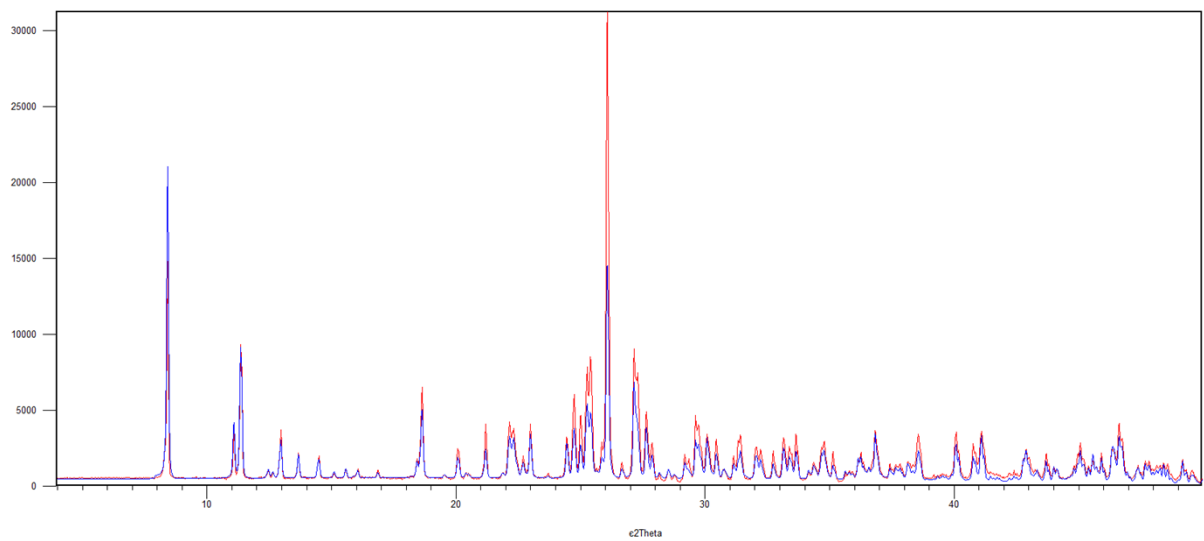


Figure S5. Experimental powder XRD of **4** (red) in comparison with the pattern simulated from single crystal X-ray data for **4** (black).

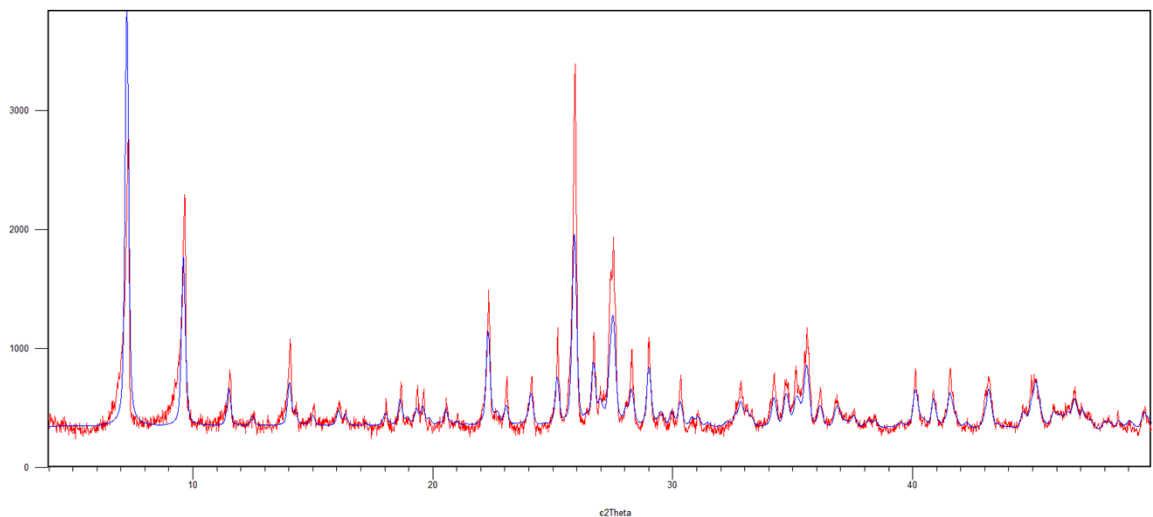


Figure S6. Experimental powder XRD of **5** (red) in comparison with the pattern simulated from single crystal X-ray data for **5** (black).

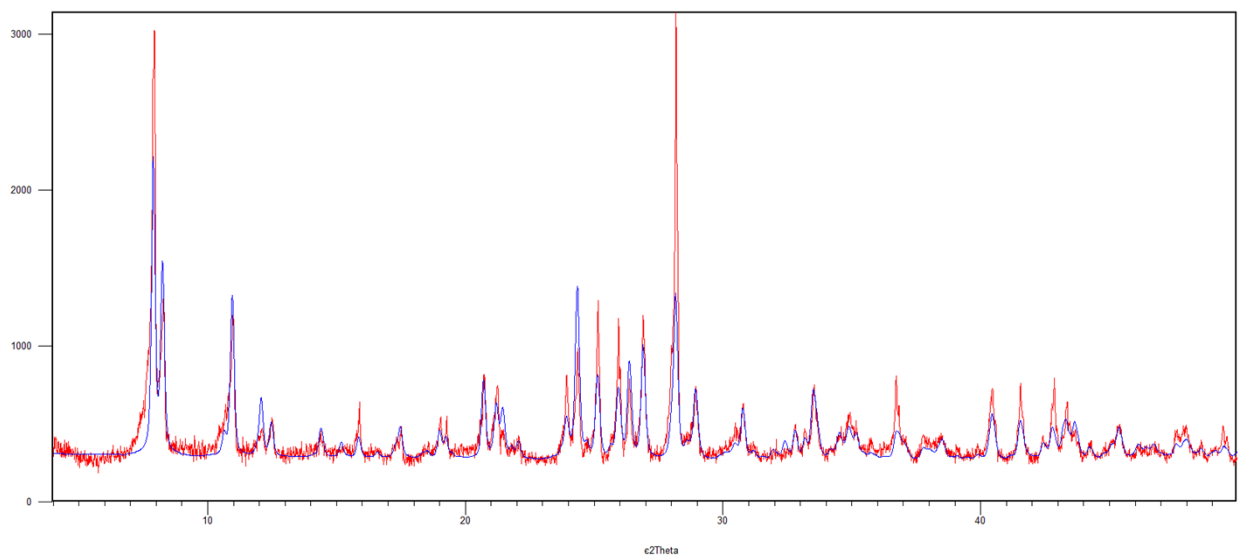


Figure S7. Experimental powder XRD of **6** (red) in comparison with the pattern simulated from single crystal X-ray data for **6** (black).

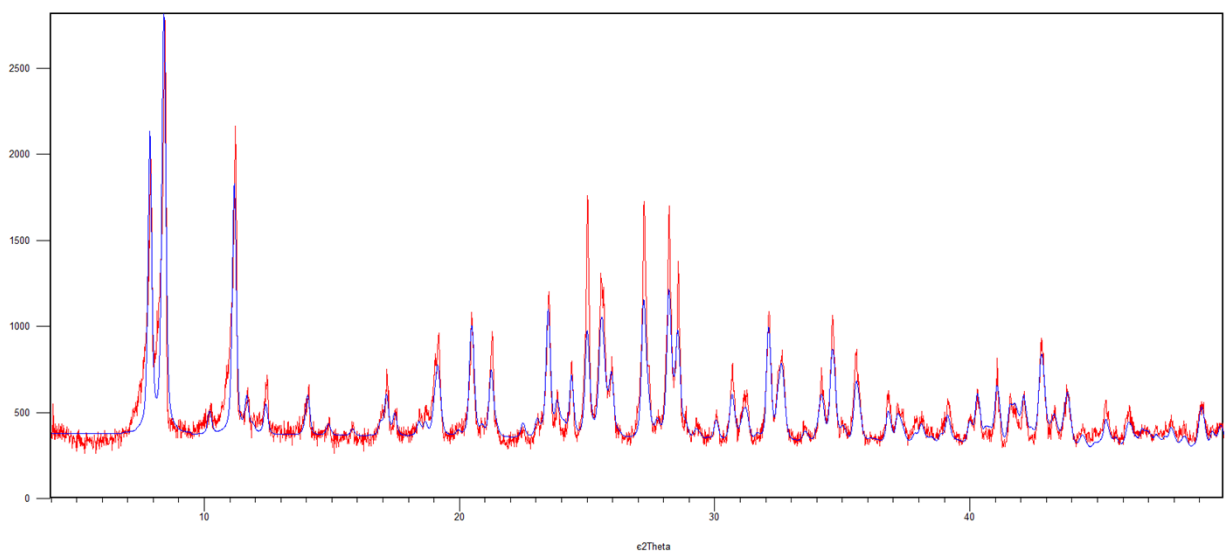


Figure S8. Experimental powder XRD of **7** (red) in comparison with the pattern simulated from single crystal X-ray data for **7** (black).

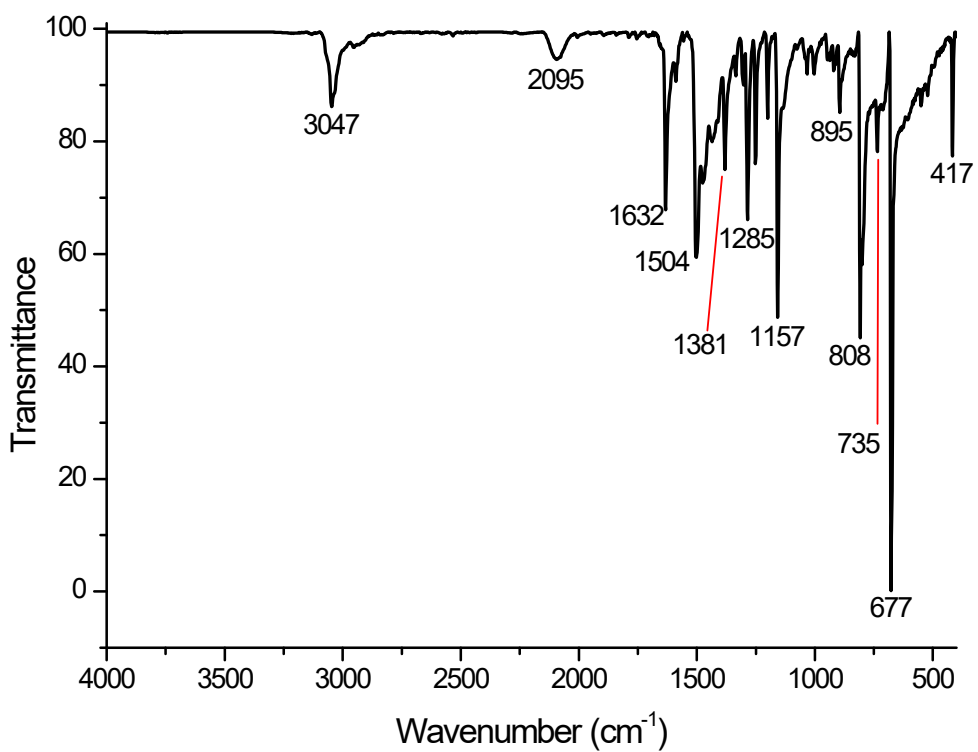


Figure S9. FTIR spectrum of **1**.

FT-IR **1** ( $\text{cm}^{-1}$ ): 3047 (w), 2095 (w), 1632 (s), 1504 (m), 1381 (w), 1285 (m), 1157 (m), 895 (w), 808 (m), 735 (w), 677 (s), 417 (w).

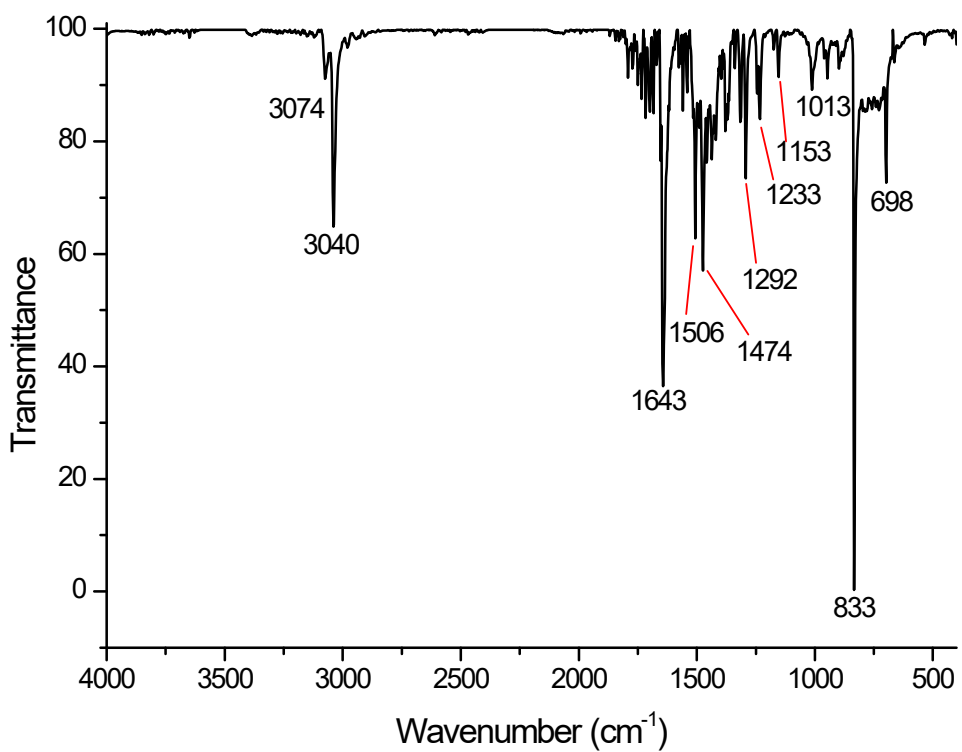


Figure S10. FTIR spectrum of **2**.

FT-IR **2** ( $\text{cm}^{-1}$ ): 3074 (w) 3040 (m), 1643 (m), 1506 (m), 1474 (m), 1292 (w), 1233 (w), 1153 (w), 1013 (w), 833 (s), 698 (w).

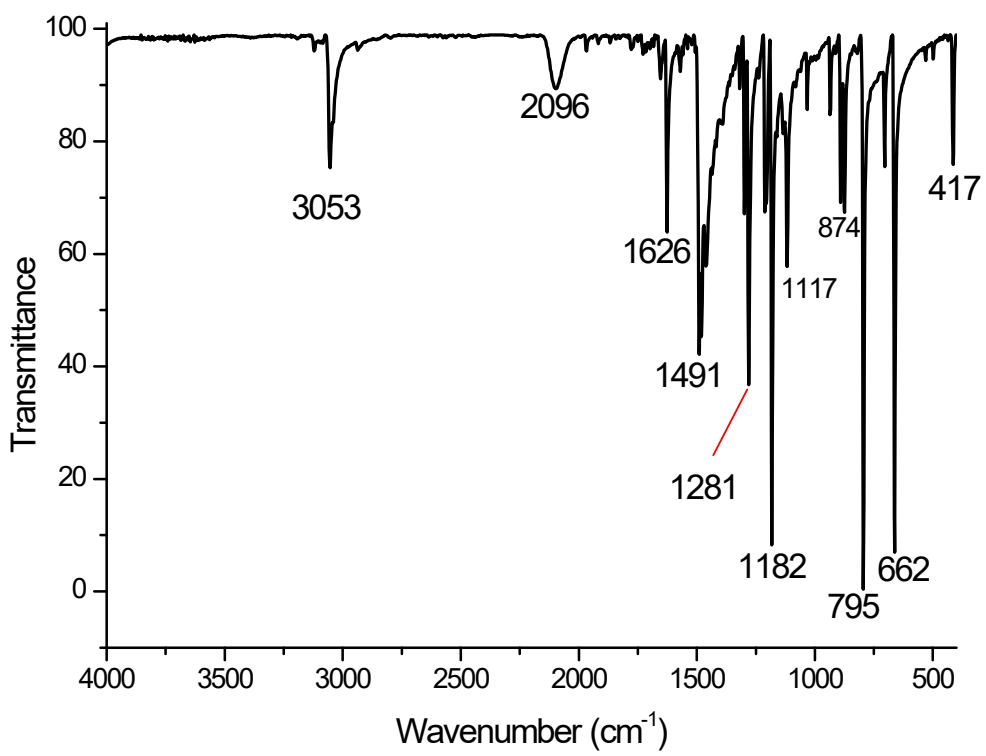


Figure S11. FTIR spectrum of **3**.

FT-IR **3** ( $\text{cm}^{-1}$ ): 3053 (w), 2096 (w), 1626 (s), 1491 (m), 1281 (w), 1182 (m), 1117 (m), 874 (w), 795 (m), 662 (w), 417 (w).

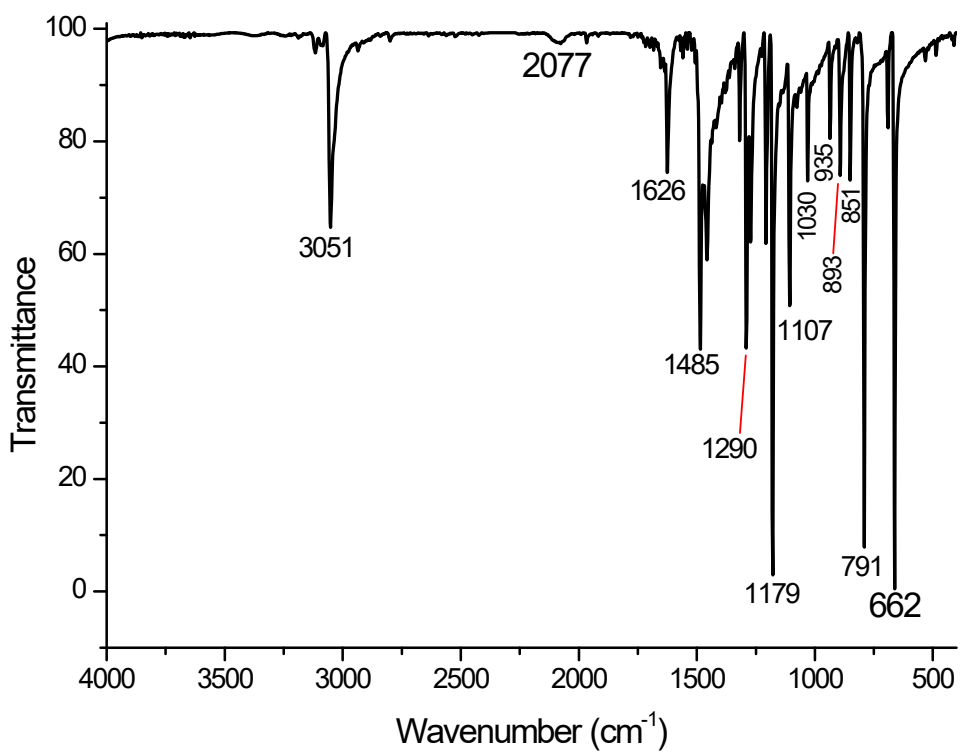


Figure S12. FTIR spectrum of **4**.

FT-IR **4** ( $\text{cm}^{-1}$ ): 3051 (m), 2077 (w), 1626 (s), 1485 (m), 1290 (m), 1179 (s), 1117 (m), 1107 (m), 1030 (w), 935 (w), 893 (m), 851 (m), 791 (s), 662 (s).

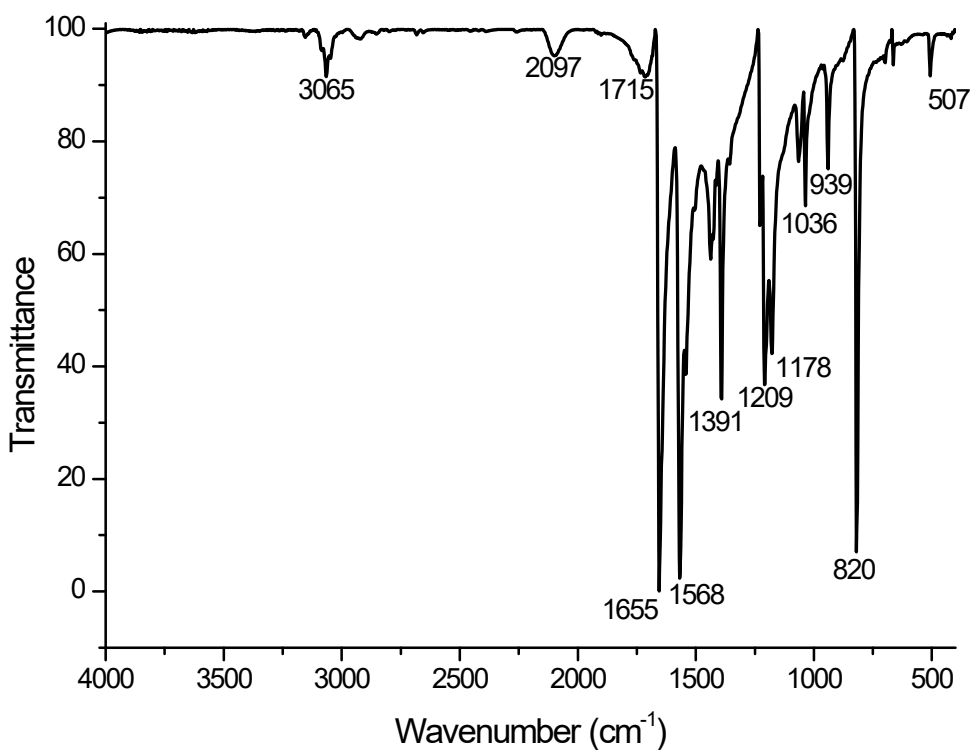


Figure S13. FTIR spectrum of **5**.

FT-IR **5** ( $\text{cm}^{-1}$ ): 3065 (w), 2097 (w), 1715 (ww) 1655 (s), 1568 (s), 1391 (m), 1209 (m), 1178 (m), 1036 (m), 939 (w), 820 (s), 507 (w).

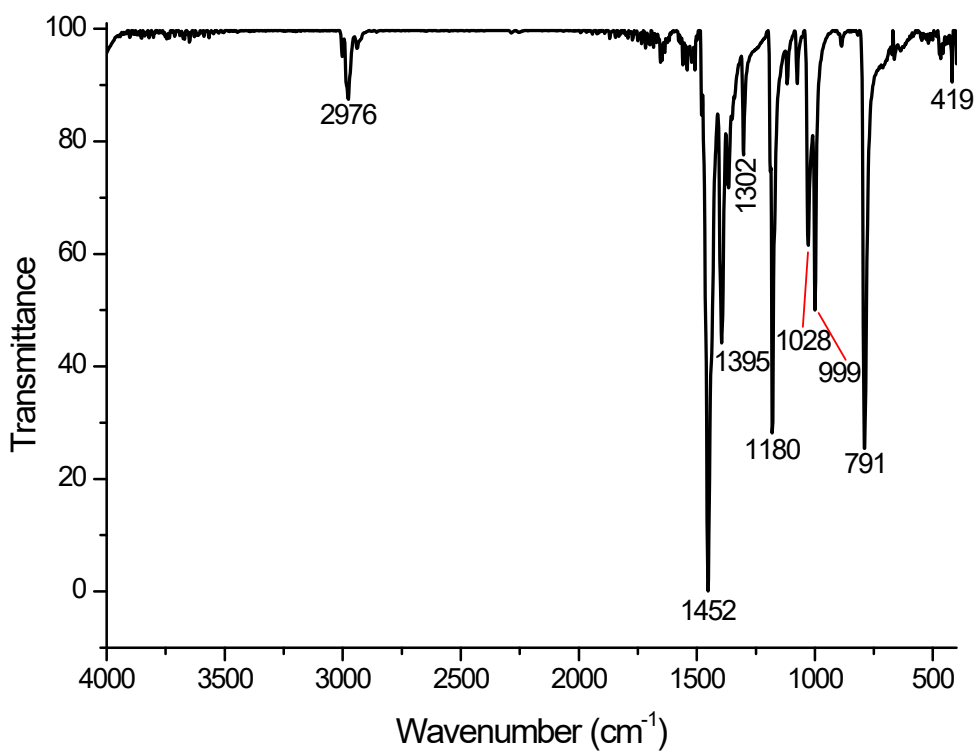


Figure S14. FTIR spectrum of **6**.

FT-IR **6** ( $\text{cm}^{-1}$ ): 2976 (w), 1452 (s), 1395 (m), 1302 (w), 1180 (m), 1028 (m), 999 (m), 791 (m), 419 (w).

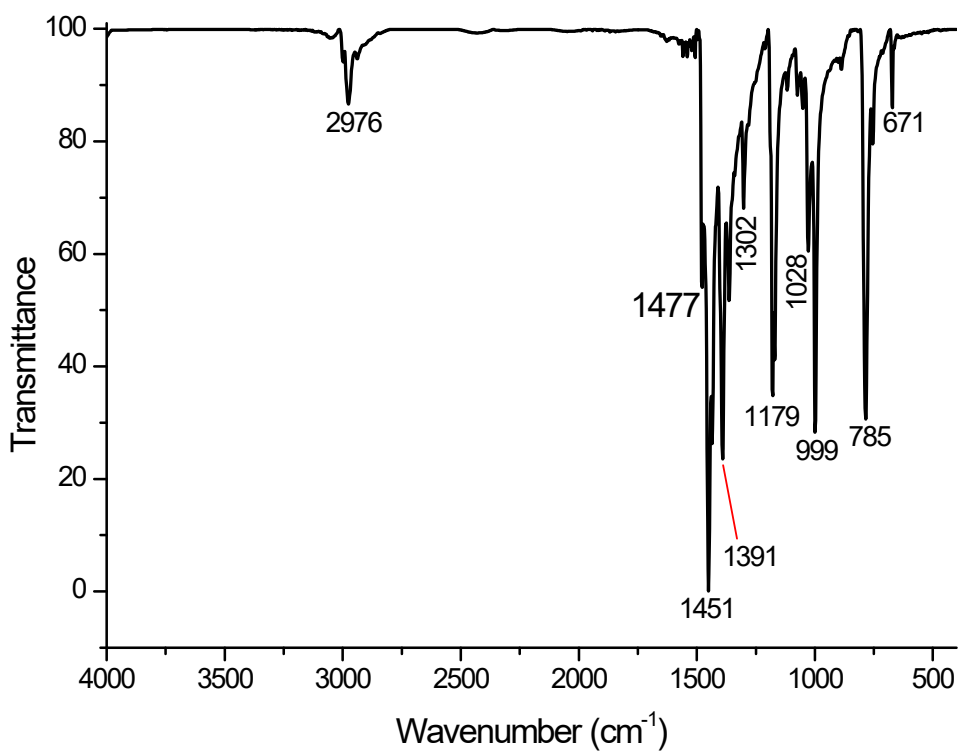


Figure S15. FTIR spectrum of 7.

FT-IR 7 ( $\text{cm}^{-1}$ ): 2976 (w), 1477 (m), 1451 (s), 1391 (m), 1302 (w), 1179 (m), 1028 (m), 999 (m), 785 (m), 671 (w).

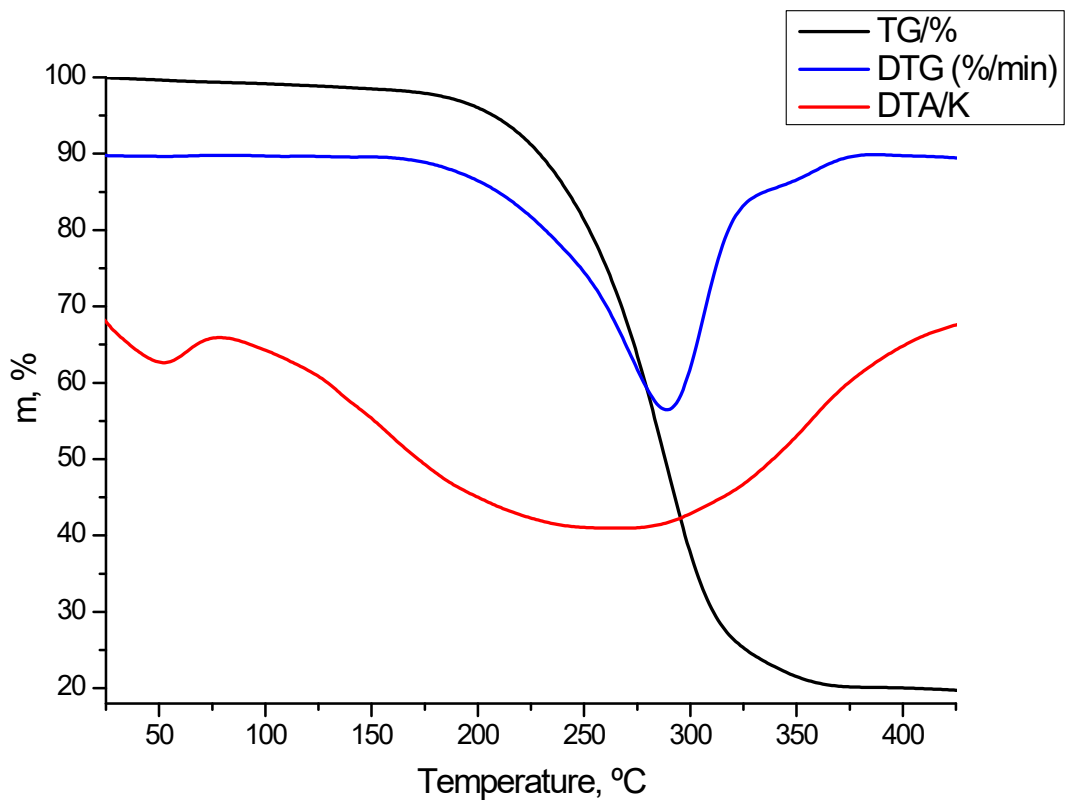


Figure S16. TG, DTG and DTA curves for **1**.

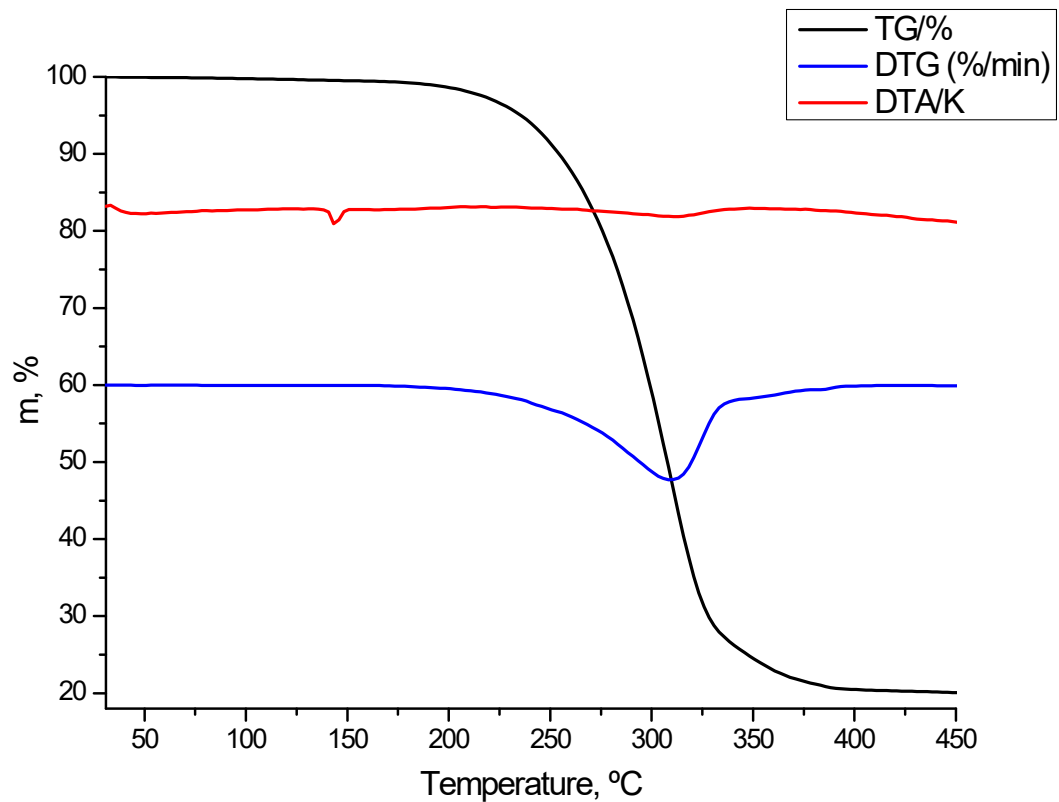


Figure S17. TG, DTG and DTA curves for **2**.

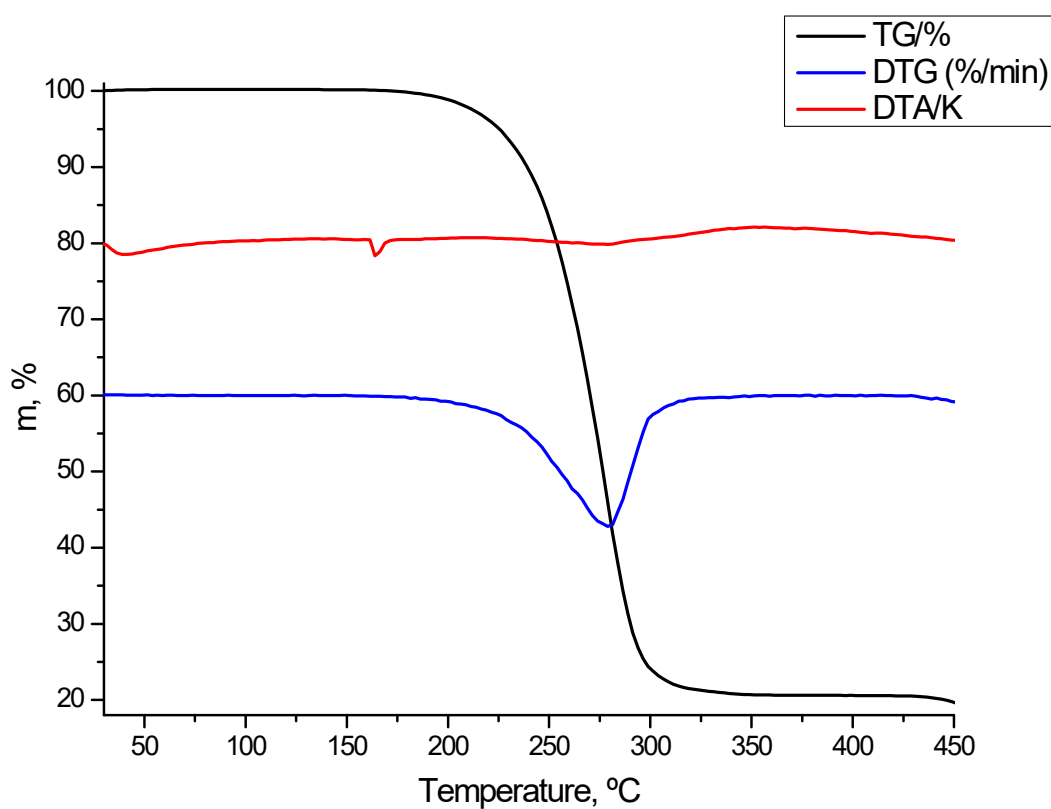


Figure S18. TG, DTG and DTA curves for **3**.

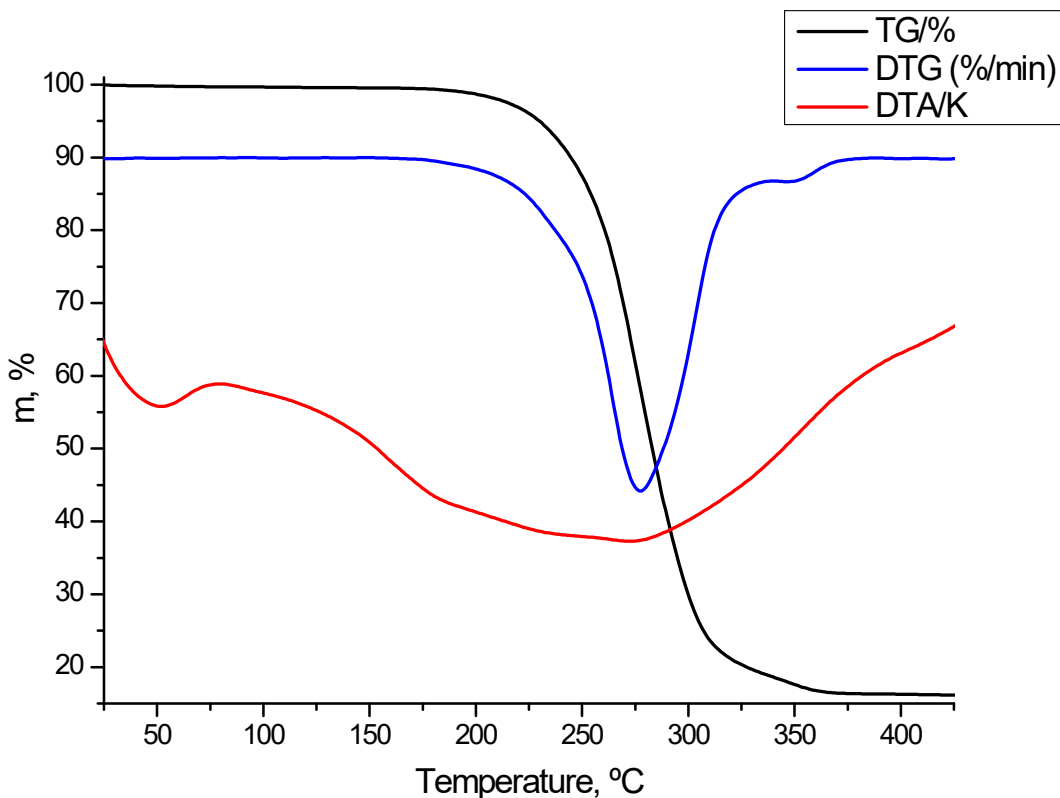


Figure S19. TG, DTG and DTA curves for **4**.

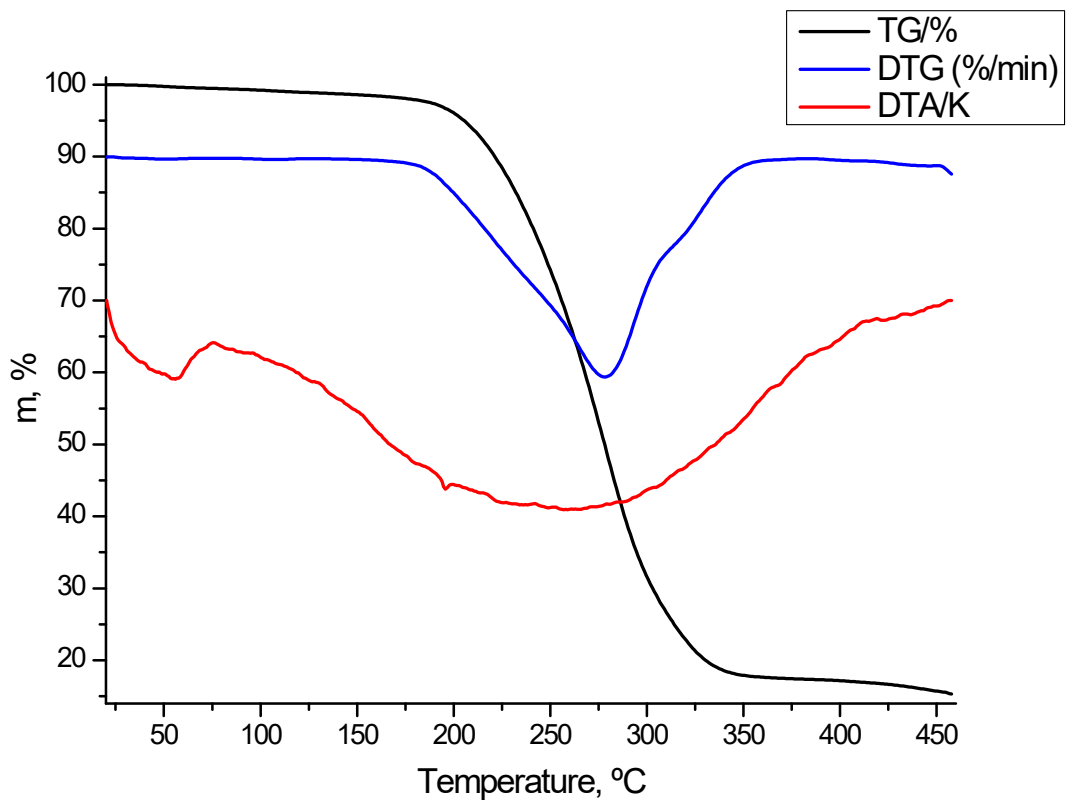


Figure S20. TG, DTG and DTA curves for **6**.

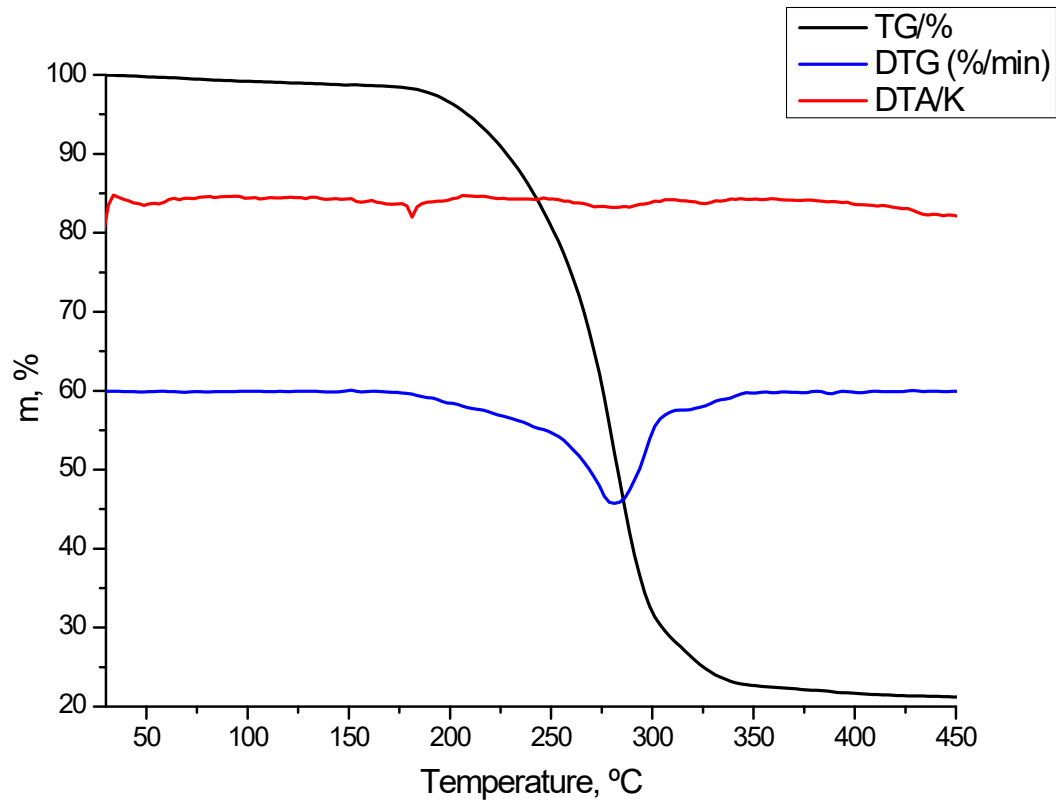


Figure S21. TG, DTG and DTA curves for **7**.

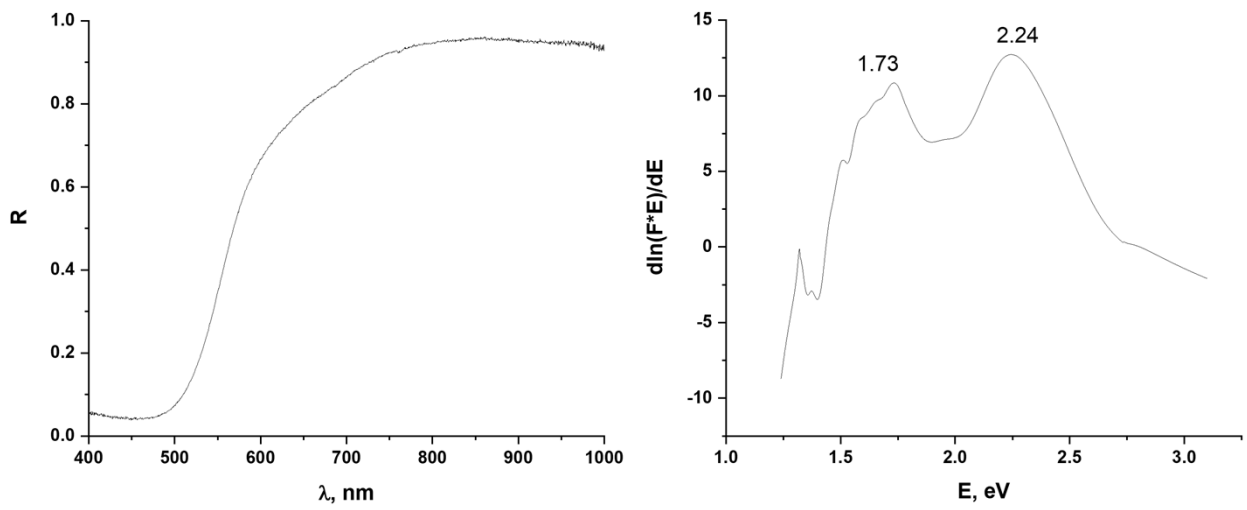


Figure S22. Diffuse reflectance spectrum (*left*) and band gap determination (*right*) for **2**.

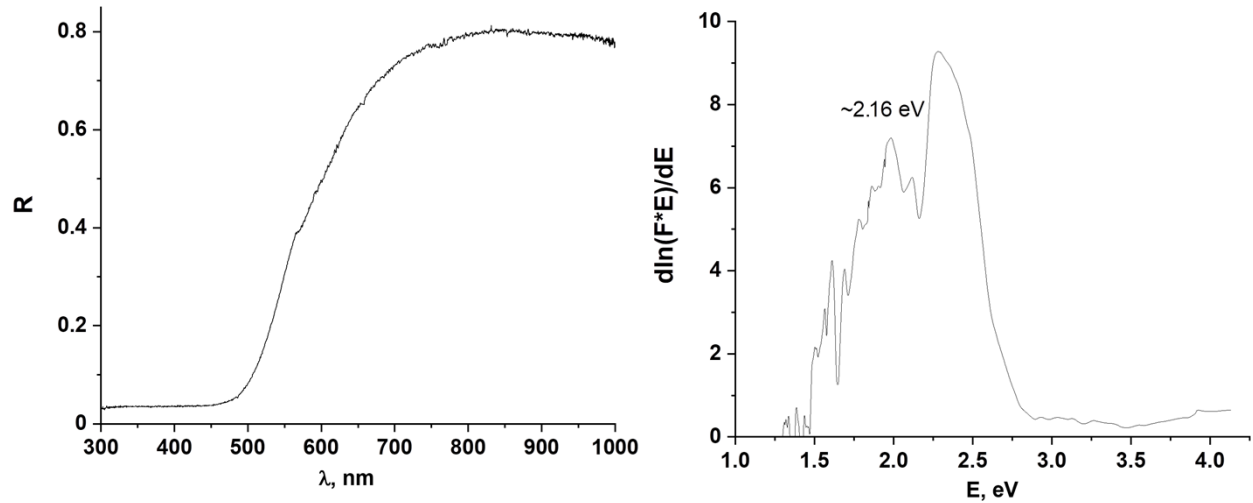


Figure S23. Diffuse reflectance spectrum (*left*) and band gap determination (*right*) for **3**.

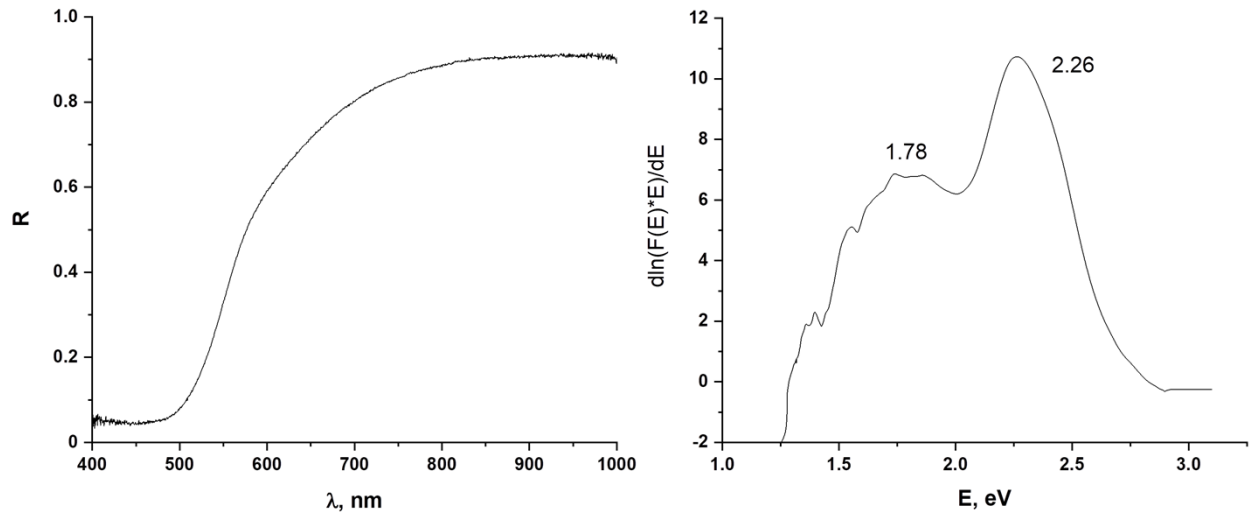


Figure S24. Diffuse reflectance spectrum (*left*) and band gap determination (*right*) for **4**.

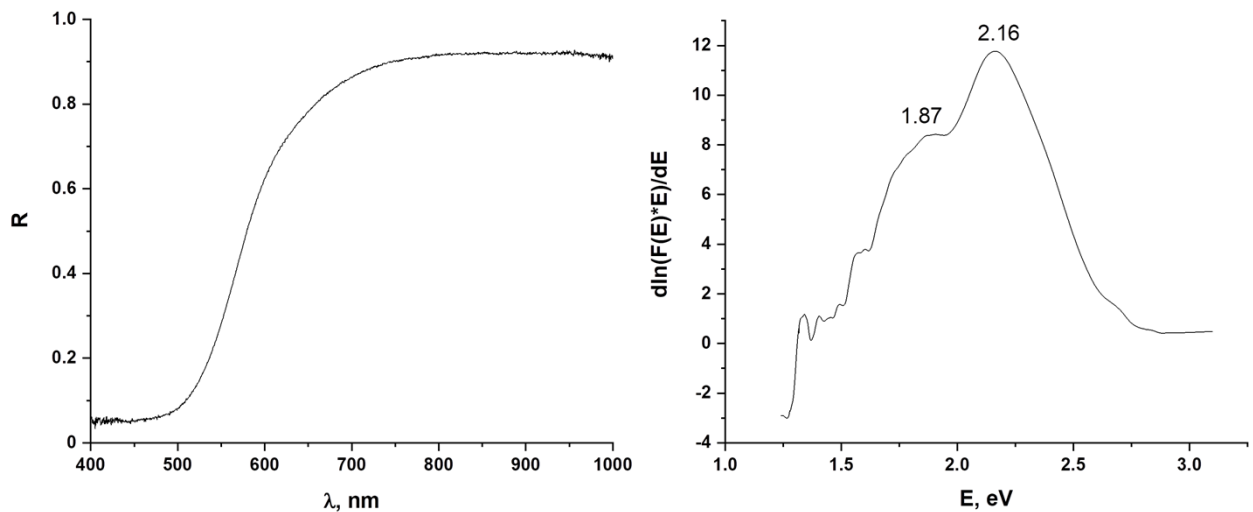


Figure S25. Diffuse reflectance spectrum (*left*) and band gap determination (*right*) for **5**.

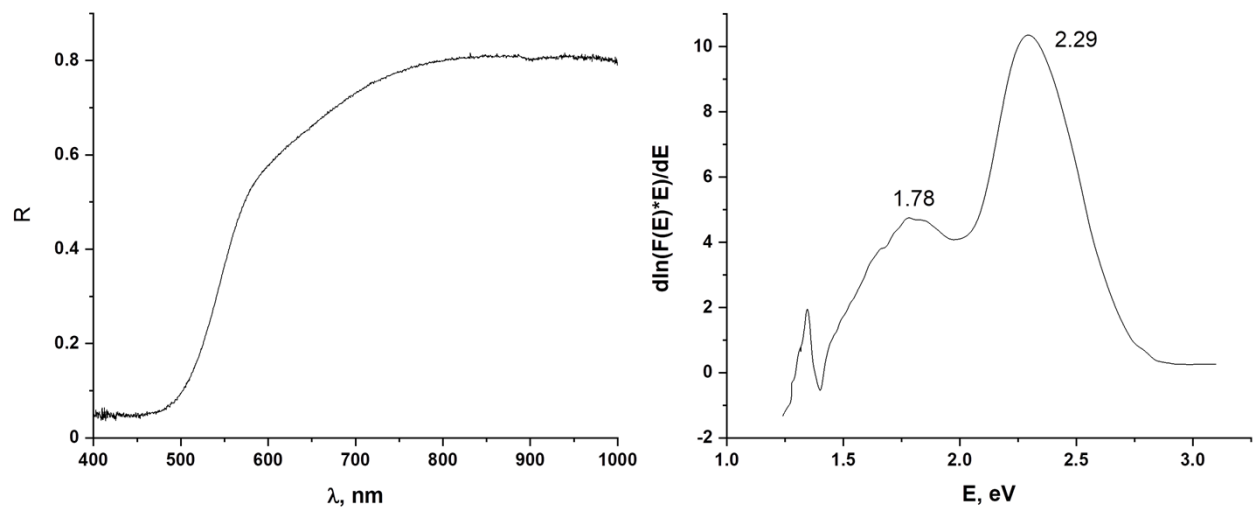


Figure S26. Diffuse reflectance spectrum (*left*) and band gap determination (*right*) for **6**.

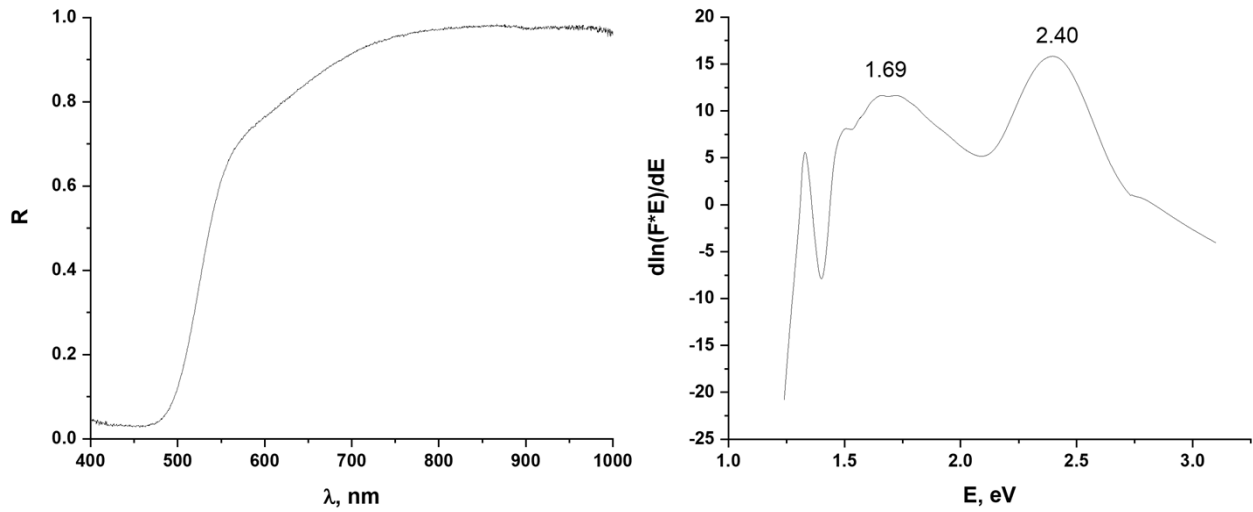


Figure S27. Diffuse reflectance spectrum (*left*) and band gap determination (*right*) for **7**.